Liquid Crystals
Publication details, including instructions for authors and subscription information:
http://www.informaworld.com/smpp/title~content=t713926090

Structures and properties of dendrimers having peripheral 2,3-difluorobiphenyl mesogenic units: effects of dendrimer generation

Osamu Haba[a]; Ken-Ichi Okuyama[a]; Hirotomo Osawa[a]; Koichiro Yonetake[a]
[a] Department of Polymer Science and Engineering, Faculty of Engineering, Yamagata University, 3-4-16, Jonan, Yonezawa 992-8510, Japan

To cite this Article Haba, Osamu , Okuyama, Ken-Ichi , Osawa, Hirotomo and Yonetake, Koichiro(2005) 'Structures and properties of dendrimers having peripheral 2,3-difluorobiphenyl mesogenic units: effects of dendrimer generation', Liquid Crystals, 32: 5, 633 — 642
To link to this Article: DOI: 10.1080/02678290500117332
URL: http://dx.doi.org/10.1080/02678290500117332

Liquid Crystals, Vol. 32, No. 5, May 2005, 633–642

Structures and properties of dendrimers having peripheral 2,3-difluorobiphenyl mesogenic units: effects of dendrimer generation

OSAMU HABA*, KEN-ICHI OKUYAMA, HIROTOMO OSAWA and KOICHIRO YONETAKE

Department of Polymer Science and Engineering, Faculty of Engineering, Yamagata University, 3-4-16, Jonan, Yonezawa 992-8510, Japan

(*Received 1 November 2004; accepted 9 January 2005*)

1st–5th generation poly(propyleneimine) dendrimers having peripheral 2,3-difluorobiphenyl mesogenic groups have been synthesized. They exhibited smectic liquid crystalline behaviour. All the liquid crystalline dendrimers exhibited a smectic A (SmA) phase and a crystal E (E) phase. The SmA–isotropic phase transition temperature increased with increasing generation. In addition, a homeotropic structure was spontaneously formed on a glass plate in the SmA phase for the 2nd, 3rd, and 4th generation dendrimers. The hometropic structure remained unchanged in the phase.

1. Introduction

Dendrimers that are highly branched three-dimensional macromolecules are attracting increasing attention because of their unique structures and properties [1−3]. They possess well defined branched structures and show low solution and bulk viscosities compared with linear or branched polymers, due to the absence of entanglements. The large number of reactive end groups existing at the periphery of dendrimers react easily with many reagents to give dendrimers with various functionalities. Therefore, they are receiving interest as new polymeric materials for applications such as catalysts, antenna for photo-induced energy, chiral recognition and enantiomer separation, unimolecular micelles, drug delivery and molecular electronics [4−8].

A dendrimer prepared by the convergent synthesis of racemic AB_2 rod-like mesogenic dendrons was reported to exhibit thermotropic nematic and smectic liquid crystalline phases [9]. Ponomarenko *et al.* [10] and Lorenz *et al.* [11] independently reported carbosilane-based liquid crystalline dendrimers, made by introducing various mesogenic units as end groups. These materials were shown to display smectic mesophases; their low viscosities and relatively low phase transition temperatures may be attributed to the dendritic topology. Thus, dendritic liquid crystalline polymers appear promising materials for optical switching and electro-optical applications. Furthermore, a dendritic aliphatic polyester functionalized with a ferroelectric mesogen has been reported to show a ferroelectric smectic C* (SmC*) phase: ferroelectric switching was observed in the phase on applying an a.c. electric field [12]. Thus, the structure and properties of liquid crystalline dendrimers are very interesting areas of research because dendrimers are already showing promise as exciting well defined building blocks in the design of new liquid crystals.

We have reported the synthesis and characterization of poly(amidoamine)-based and poly(propyleneimine)-based liquid crystal dendrimers with rigid cyanobiphenyl mesogens coupled by amide linkages [13, 14]. They showed lyotropic liquid crystallinity in DMF solution, but did not show thermotropic liquid crystallinity. This is because the amide bond strongly influences the rigidity of dendrimers through strong intermolecular hydrogen bonding. Thus, liquid crystal dendrimers were derived from poly(propyleneimine) dendrimers coupled with cyanobiphenyl or 2,3-dicyanophenyl mesogens by ester linkages [15, 16]. They exhibited thermotropic liquid crystallinity, specifically a smectic A (SmA) phase. The temperature range of the smectic phase increased on increasing the generation number of the dendritic core and the length of the flexible spacers. Furthermore homeotropic orientations were obtained for the dendrimers with the 2nd generation scaffold, when slowly cooled or kept in the SmA phase [15]. This has been observed in other liquid crystal dendrimers [10]. An orientation perpendicular to a mica surface was formed in carbosilane dendrimers with cholesteryl mesogenic end groups [17]. In the case of amphiphilic dendrimers, stable monolayers were formed at the air–water interface [18]; it has been suggested that the

*Corresponding author. Email: haba@yz.yamagata-u.ac.jp

Liquid Crystals
ISSN 0267-8292 print/ISSN 1366-5855 online © 2005 Taylor & Francis Group Ltd
http://www.tandf.co.uk/journals
DOI: 10.1080/02678290500117332

amphiphilic chains were aligned perpendicular to the water surface, and the dendritic surfactants adopt a cylindrical shape at the interface. Thus, both liquid crystalline and amphiphilic dendrimers exhibit self-assembly properties. The behaviour of liquid crystal dendrimers depends on the dendrimer generation number and/or the terminal mesogenic structure [19–22]. However very few studies of the effect of generation number on the structures and properties of such dendrimers have been carried out. Thus, we have initiated an investigation on the structures and properties of liquid crystal dendrimers of different generations. The present paper describes the relationship between properties and generation of dendrimers having peripheral 2,3-difluorobiphenyl mesogenic units.

2. Results and discussion

2.1. *Synthesis of liquid crystalline dendrimers having difluorobiphenyl mesogenic groups (DFDs)*

Starting from 2,3-difuluorophenol (**1**) and 4-bromophenol (**4**), the target mesogenic groups having a C_{10} spacer (**8**) were prepared through six steps as shown in scheme 1. First, **1** was reacted with bromobutane to give the butyl ether (**2**), which was converted to the boronic acid (**3**). The hydroxyl group of **4** was protected with a *tert*-butyldimethylsilyl group, and then underwent Suzuki coupling with **3** to give biphenyl derivative **6**. Finally, the acrylate **8** was prepared after introducing the spacing group by reaction with 10-bromododecanol. The introduction of **8** to the commercial polypropyleneimine dendrimer

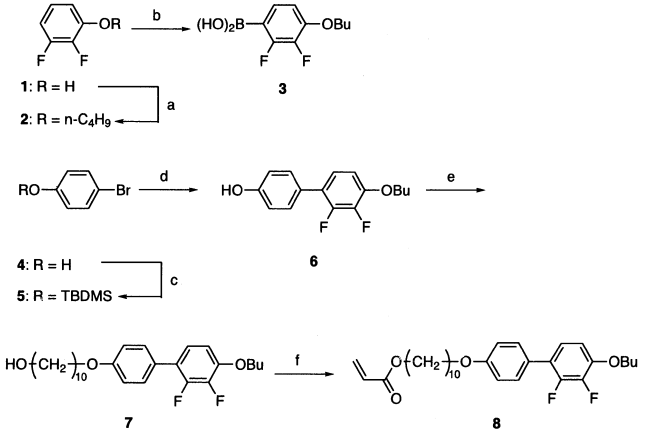

Scheme 1. Synthesis of mesogenic unit **8**. Conditions: (a) *n*-C_4H_9Br, K_2CO_3, 2-butanone, reflux; (*b*) 1) *n*-BuLi, Hexane, THF, 2) $B(OMe)_3$, THF, $-70^\circ C$, 3) HCl; (c) $(CH_3)_3CSi(CH_3)_2Cl$, DMAP, THF, r.t.; (d) 1) **3**, $Pd(PPh_3)_4$, C_6H_6, 2M Na_2CO_3 aq., reflux, 2) Bu_4NF, THF, e) HO–$(CH_2)_{10}$–Br, K_2CO_3, acetone, reflux, (f) $CH_2=CH$–COCl, Et_3N, THF, r.t.

(generation = 1–5) was achieved by Michael-type addition of the peripheral amino groups to the acrylate, as shown in scheme 2. The reaction was conducted by heating the dendrimers and **8** at 45°C in THF for 1 week, monitoring the disappearance of primary and secondary amino groups due to incomplete additions by ^1H NMR spectroscopy. The reaction mixture was poured into *n*-hexane and the precipitate filtered and washed with *n*-hexane several times to give the target dendrimers (DFD-G1–G5) as white powders.

2.2. *Determination of the structure of DFDs*

The IR spectra of all the dendrimers showed characteristic ester carbonyl and C–F bands at 1730 and 1180 cm^{-1}, respectively; no peaks at 3290–3300 cm^{-1} due to primary amino groups were observed. Figure 1 shows the ^1H NMR spectrum for DFD-G2, which has

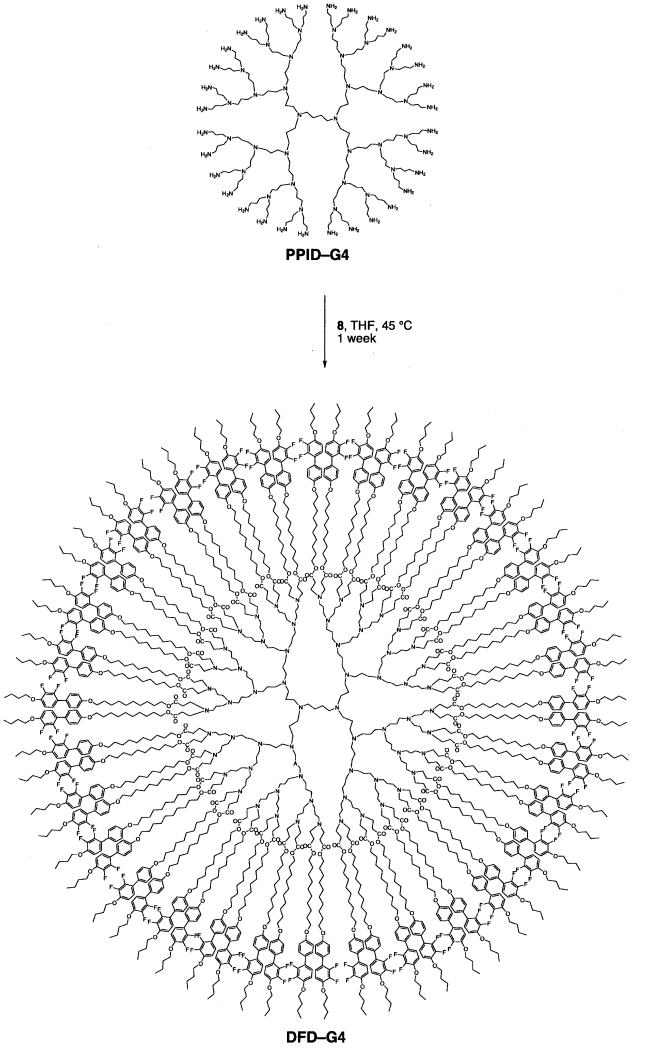

Scheme 2. Syntheses of the DFDs.

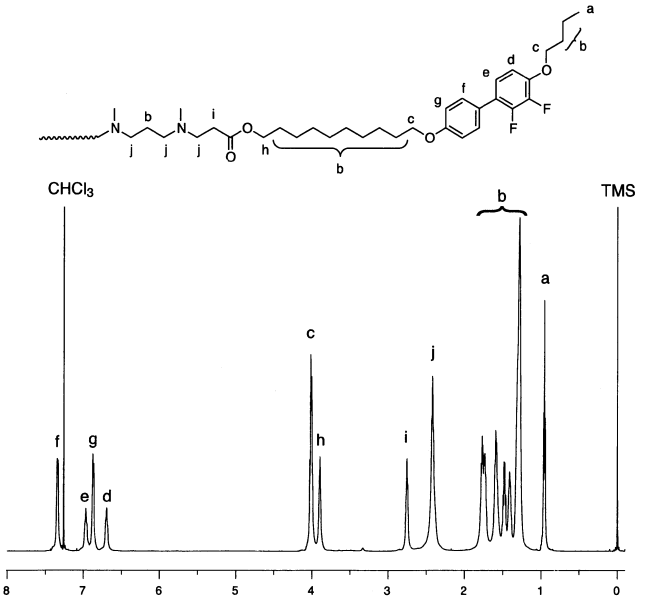

Figure 1. ^{1}H NMR spectra of DFD-G4, measured in $CDCl_3$ at r.t.

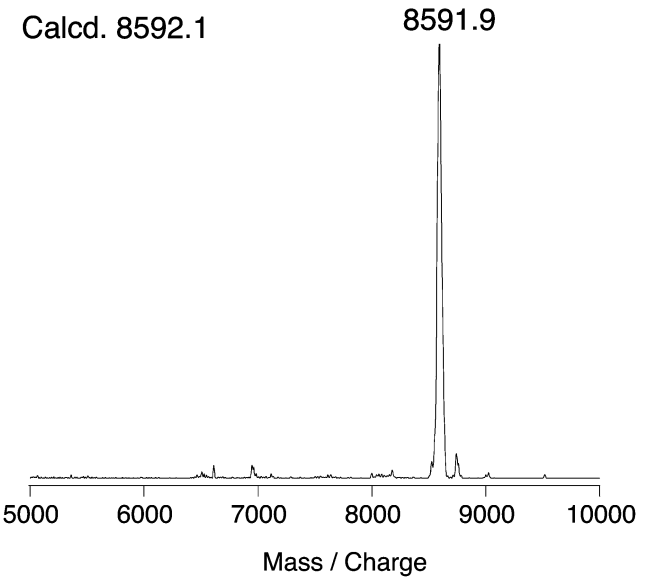

Figure 2. MALDI-TOF mass spectrum of DFD-G2. 2,5-Dihydroxybenzoic acid was used as a matrix.

16 difluorobiphenyl units at the chain ends. Some distinct features are apparent. All the protons in the structure were identified and all assignments are shown in figure 1. Other DFDs showed similar ^{1}H NMR spectra.

The molecular masses of the DFDs were determined by GPC. All the GPC chromatograms showed a clear unimodal molecular mass distribution. The relative M_n and M_w values of the DFDs are summarized in table 1. Larger dendrimers than the third generation showed a smaller molecular mass than the calculated value. This may be attributed to the spherical shape of the larger dendrimers. However, the polydispersity for all the dendrimers were very close to 1.0, implying that the DFDs have very narrow molecular mass distributions.

The MALDI-TOF mass spectrum of DFD-G2 shows one signal that is clearly due to the formation of the desired dendrimers with 16 mesogens (figure 2); DFDs of higher generation were barely ionized. The *m*/*z* value of the signal was 8591.9, which corresponds to the calculated value of 8592.1. These results are also listed in table 1 and clearly indicate the formation of the desired DFDs.

2.3. *Phase transitions of the DFDs*

The DSC traces of the DFDs obtained in the 2nd cooling cycle are given in figure 3; each contains two distinct exothermic peaks (T_1 and T_2), suggesting that two kinds of liquid crystalline phase are formed in each sample. The temperature of the exothermic peak observed at higher temperatures increased with increasing generation, while that seen at lower temperatures remained almost unchanged. The temperature range between the two exothermic peaks increased with increasing generation number.

The optical textures of the DFDs were observed by polarizing optical microscopy (POM) using crossed polarizers to identify the liquid crystalline phases.

Table 1. Molecular mass and distribution of DFDs.

	MALDI-TOF MS		GPC[a]	
Dendrimer	M+H$^+$(calcd)	M+H$^+$(found)	$M_n \times 10^{-3}$	M_w/M_n
DFD-G1	4226.42	4223.8	5.7	1.03
DFD-G2	8592.07	8591.9	8.6	1.02
DFD-G3	17323.36	—[b]	12.8	1.08
DFD-G4	34786.04	—[b]	17.5	1.08
DFD-G5	69711.08	—[b]	23.9	1.09

[a]Estimated using standard polystyrene calibration. [b]Not determined.

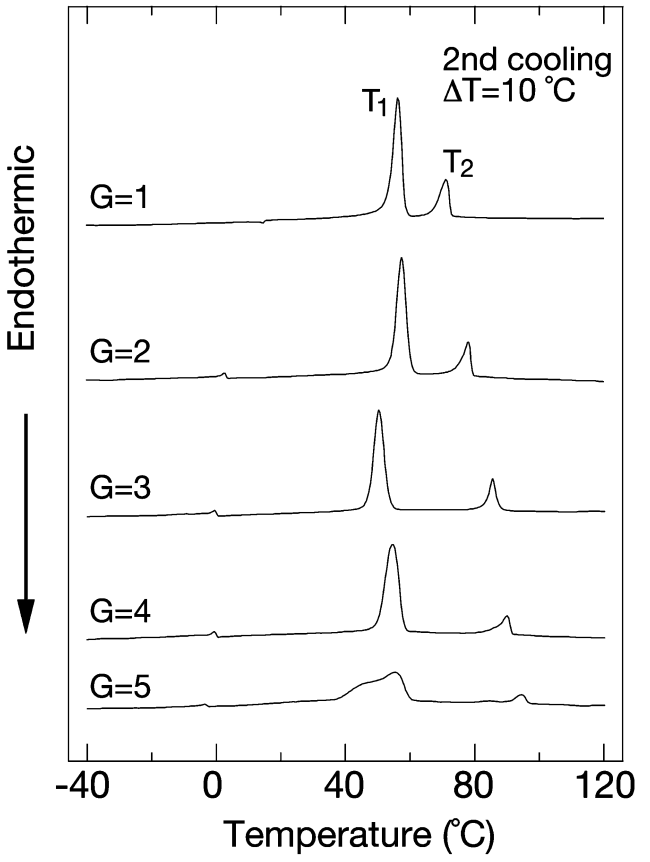

Figure 3. DSC traces of DFDs obtained on cooling.

Above T_2 the optical texture disappeared and changed to a dark field, suggesting an isotropic melt. Thus, T_2 is the clearing point. Figure 4 shows photographs of the optical textures taken at temperatures between the two exothermic peaks and at room temperature. A focal-conic fan texture was observed at temperatures between the two exothermic peaks as shown in the left-hand column in figure 4. Thus the phase was assigned as SmA. The smectic structure consists of layers in which the mesogenic units and the dendritic interior (core and flexible spacers) are separated [15, 19, 21]. The optical texture drastically changed below the lower temperature peak as shown in the right-hand column in figure 4. The focal-conic fan texture disappeared and changed into one composed of dark domains. The liquid crystalline phase may be a highly ordered smectic phase, because the exothermic peak was comparatively high and sharp. The optical retardation of the texture in the phase is very low as compared with that of the SmA phase. Such a drastic change in retardation has rarely been observed. The low retardation may be attributed to the fluorine atom having a small refractive index.

X-ray diffraction (XRD) measurements were carried out to determine the nature of the phase. The XRD

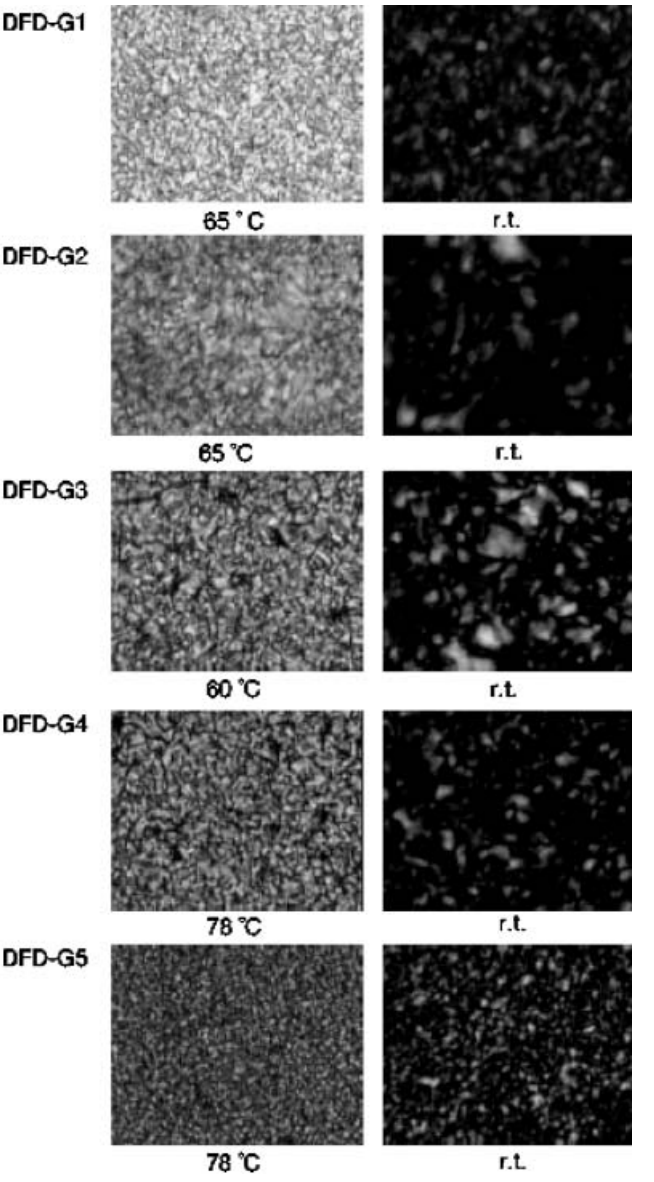

Figure 4. Polarizing optical micrographs of the DFDs.

patterns are shown in figure 5. The patterns in the left-hand and the right-hand columns were taken in the higher and lower temperature phases, respectively. The XRD patterns for the higher temperature phase showed Debye–Sherrer rings in the small angle and a diffuse halo at wide angle. The small angle reflections are due to the smectic layer structure. The diffuse reflection at wide angle was observed at approximately 0.45 nm, which corresponds to the lateral distance between the mesogens. These results confirmed that the liquid crystalline phase is SmA.

By contrast comparatively sharp Debye-Sherrer rings appeared at wide angles in the XRD patterns of the lower temperature phase, as shown in the right-hand

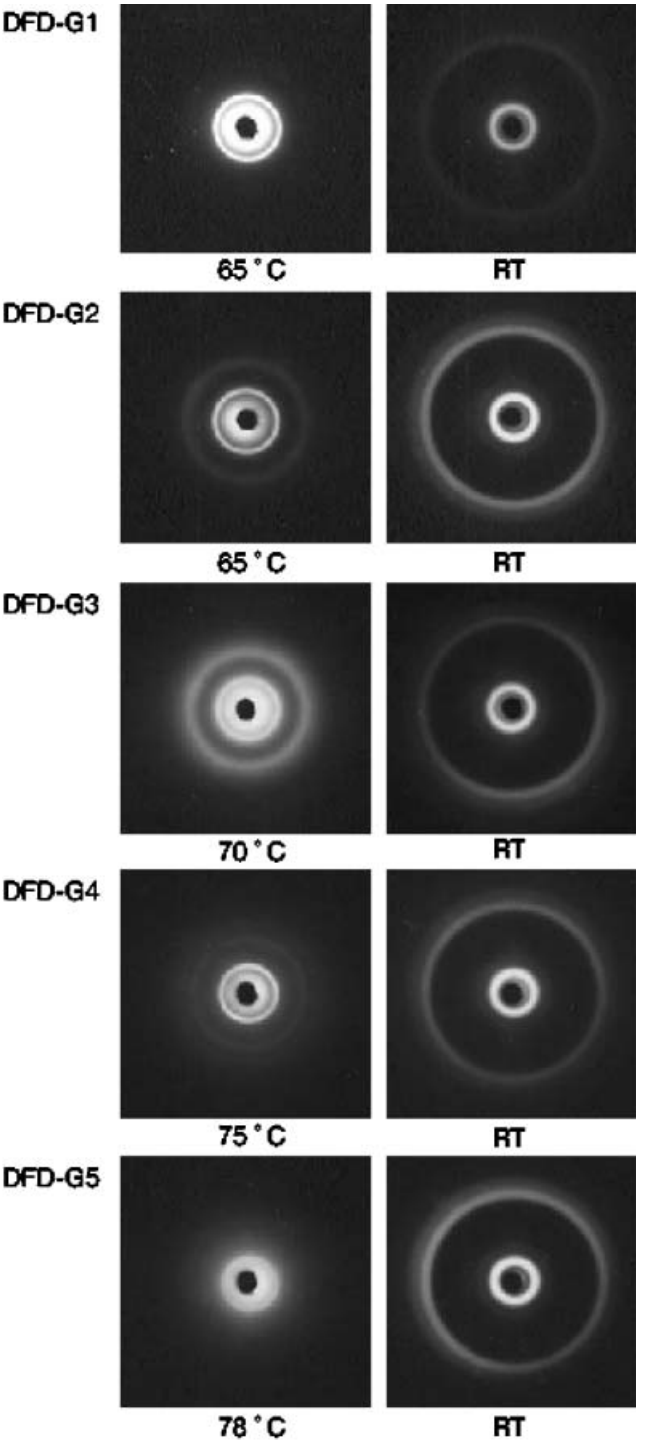

Figure 5. X-ray diffraction patterns of the DFDs.

column in figure 5. The *d*-spacing values of the three wide angle reflections were estimated. They are not consistent with hexagonal packing and thus the phase is not assigned as a hexatic smectic B. The three reflections, however could be assigned as the (1 1 0), (2 0 0) and (2 1 0) reflection consistent with an orthorhombic packing; the lattice parameters, *a* and *b*, were estimated from *d*-spacings of the three reflections as shown in table 2. Thus, the lower temperature mesophase is assigned as a crystal E (E).

Table 2. Lattice parameters of the phase seen for the DFDs.

Dendrimer	*a*	*b*
DFD-G1	8.54	5.51
DFD-G2	8.54	5.60
DFD-G3	8.32	5.57
DFD-G4	8.52	5.52
DFD-G5	8.46	5.50

2.4. *Dependence of liquid crystal properties on dendrimer generation number*

The phase transition temperatures of DFDs measured on cooling are plotted against generation in figure 6. The temperature of the SmA–E phase transition remains essentially unchanged with increasing generation number. On the other hand, the temperature of the I–SmA phase transition increased with increasing generation number, indicating an expansion of the SmA temperature region. This behaviour results from the increase in the number of terminal mesogenic groups bound to the molecule with increasing generation; that

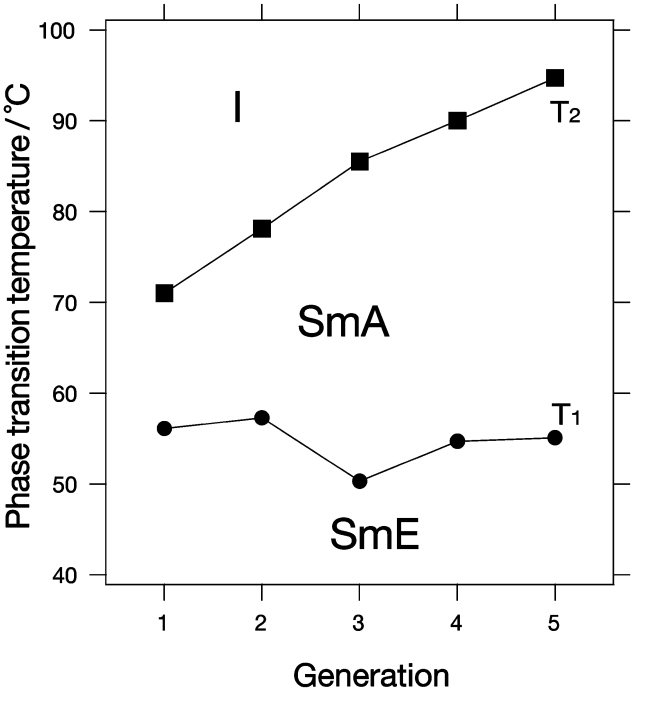

Figure 6. Relationship between phase transition temperatures and DFD generation.

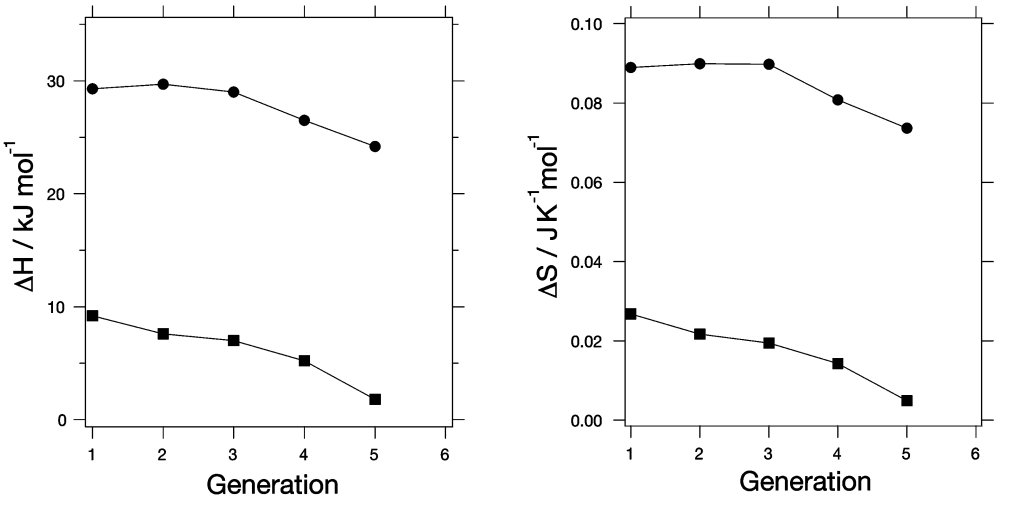

Figure 7. Relationship between enthalpy change (ΔH) and entropy change (ΔS) to the DFD generation.

is, the increase in the number of terminal mesogens enhances their cooperative interactions. This behaviour is similar to that of poly(propyleneimine)dendrimers [19] and carbosilane liquid crystalline dendrimers [21].

The enthalpy and entropy changes (ΔH and ΔS) of the I–SmA phase transition are shown in figure 7. In general, the ΔH value correlates with the volume of the smectic structure in a sample, slightly decreasing with increasing generation number. The dedrimer core binds mesogens at the periphery, and their shape becomes increasingly spherical with increasing generation. The higher generation DFDs possibly hinder the terminal mesogens entering into the smectic layer structure; this opposes the ordering of mesogenic groups into semectic layers and reduces the anisotropy of the system [21]. The less defined optical texture formed in DFD-G5 shown in figure 4 supports this view. Thus, ΔH and ΔS of the I–SmA phase transition decreased.

Figure 8 shows the relationship between the smectic layer spacing and dendrimer generation number. The layer spacings were estimated from the small angle X-ray reflections, and increased with increasing generation. Thus, the increase in layer spacing results from the increase in branching units. The DFD is probably cylindrical in the smectic phase [15, 20, 21]. Smectic structures have been observed in other liquid crystalline dendrimers [21].

2.5. *Homeotropic DFD orientation*

Figure 9 shows the optical textures of DFD-G3 slowly cooled at $1^{\circ}C\,min^{-1}$ from the isotropic melt. The fan texture disappeared, and the area of dark field gradually expanded with cooling. A typical conoscopic pattern observed at the dark field area, is shown in figure 9. This suggests that a homeotropic orientation is formed in the sample, in which the mesogens are aligned perpendicular to the glass substrate. Liquid crystalline dendrimers tend spontaneously to form a homeotropic structure on the substrate [10, 16]. We have also reported that homeotropic orientations were formed in liquid crystalline dendrimers with cyanobiphenyl mesogens [15], and suggested that the mesogens were perpendicular on the glass surface. The terminal cyano group is highly polar and binds easily to polar groups

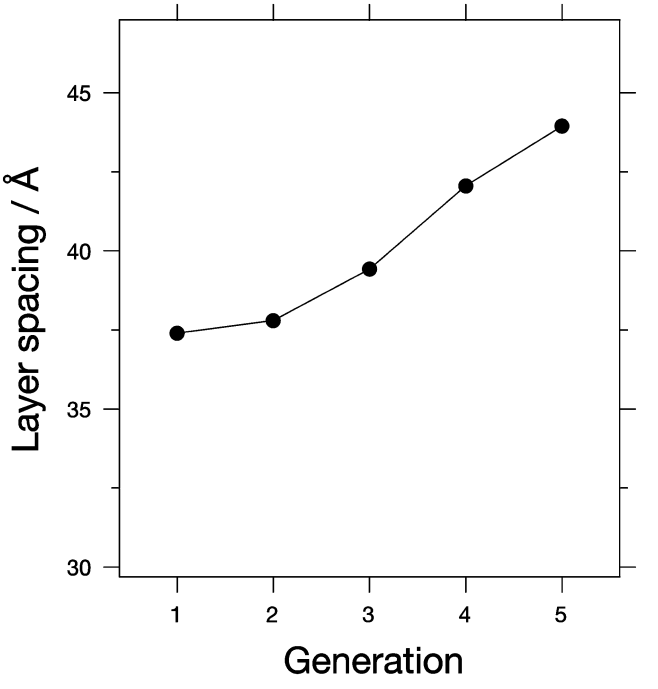

Figure 8. Change in smectic A layer spacing with DFD generation.

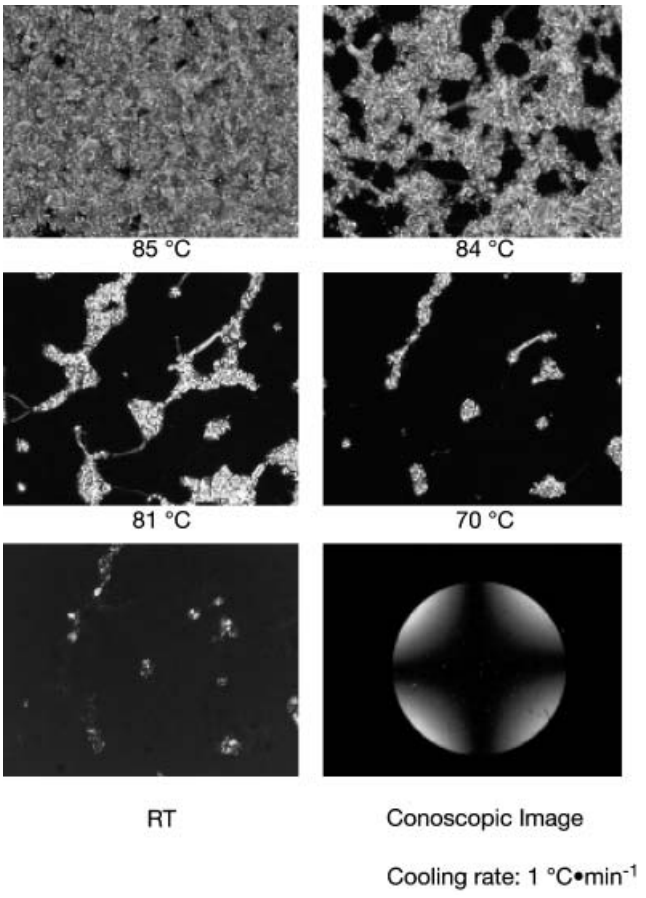

Figure 9. Polarizing optical micrographs of DFD-G3 at 85°C.

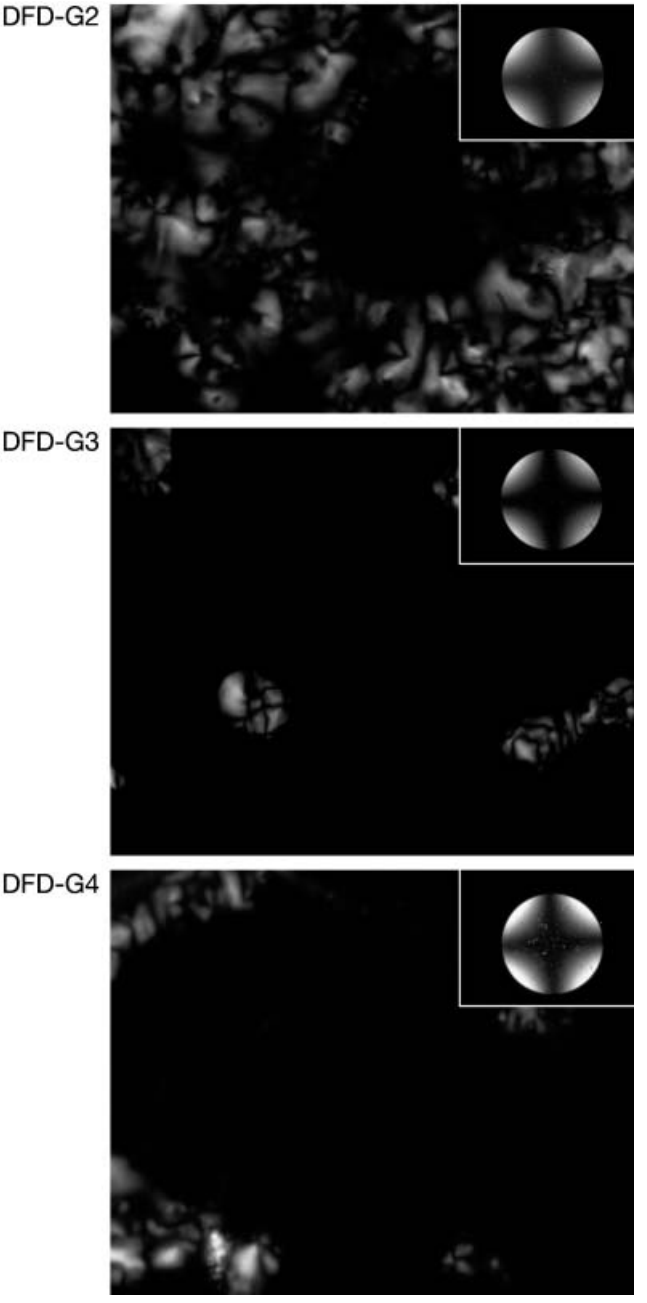

Figure 10. Optical textures and conoscopic images of DFD-G2, DFD-G3 and DFD-G4 taken at r.t.

on the glass surface. In addition, the cylindrical structure of the liquid crystalline dendrimers might give a homeotropic orientation. On the other hand, the mesogens here have no terminal cyano groups, instead they have two fluorine atoms on the side of the biphenyl groups and the strong repulsive force between these probably results in the mesogen arrangement on the glass substrate, even though it was not treated for homeotropic orientation.

Homeotropic structures were formed in DFD-G2, DFD-G3 and DFD-G4 as shown in figure 10. By contrast, no homeotropic orientation has been observed for DFD-G1 and DFD-G5. This suggests that spontaneous homeotropic orientation depends on the steric shape of liquid crystalline dendrimers. The liquid crystalline dendrimers having peripheral mesogens tend to form a cylindrical shape, and this leads to a smectic structure as described already [15, 20, 21]. It is difficult, however, for DFD-G1 to form a cylindrical shape, because there are only four terminal mesgens within the molecule. The dendritic backbone of DFD-G5, on the other hand, adopted a distorted conformation, because of the large number of branching units. The increase in the number of terminal mesogens opposes the ordering of the mesogenic groups into semectic layers, and the shape becomes increasingly spherical as described already. Thus, the steric shapes of DFD-G1 and DFD-G5 probably hindered them from forming homeotropic orientations.

3. Conclusions

DFDs with a flexible dendritic scaffold were successfully synthesized from poly(propyleneimine) dendrimers (generation 1–5) and 4-butoxy-2,3-difluoro-4′-(10-acryloyloxydecyloxy)biphenyl. The DFDs showed smectic liquid crystalline behaviour, exhibiting E and SmA phases. The I–SmA phase transition temperature increased with increasing generation number, while the SmA–E transition temperature remained essentially constant. The SmA layer specing of the increased DFDs with increasing generation number. Homeotropic orientation on a glass substrate spontaneously occurred in DFD-G2, DFD-G3, and DFD-G4; and persisted in the E phase. These properties of DFDs are of interest in the field of self-assembling materials.

4. Experimental

4.1. *Measurements*

Infrared spectra were recorded on a Horiba FT-210 spectrometer, and the NMR spectra on a Jeol LA-600 spectrometer. Differential scanning calorimetry was recorded on a Seiko SSC/5200 (DSC 220) instrument at heating/cooling rates of $10^{\circ}C\,min^{-1}$ under nitrogen. Gel permeation chromatography was carried out using polystyrene as the standard on a Jasco TRIROTAR-III HPLC equipped with a Shodex KF-80M column at 40°C in tetrahydrofuran (THF). Matrix-assisted laser desorption ionization time-of-flight ultraviolet mass spectroscopy (MALTI-TOF) was performed on a PE Biosystems Voyeger-DE Pro spectrometer using 2,4-dihydroxybenzoic acid as a matrix. Optical textures of the samples were examined using a polarizing optical microscope equipped with a hot stage (Linkam Co., TH-600RMS) under nitrogen. X-ray diffraction experiments were carried out on a RAD-rA diffractometer (Rigaku Denki Co. Ltd.) equipped with a heating device. Nickel-filtered CuK_{α} radiation was employed. Wide angle X-ray scattering (WAXS) traces were recorded by a scintillation counter system with a 1.0 mm diameter pinhole collimator and $1 \times 1^{\circ}$ receiving slit. The diffractometry was performed in transmission. The WAXS traces were obtained by a step-scanning method: step width and fixed time were programmed for steps of 0.05° every 10 s. The XRD photographs were taken by a flat Laue camera with a 0.5 mm diameter pinhole collimator.

4.2. *Materials*

2,3-Difluorophenol (Tokyo Kasei), 1-bromobutane (Kanto Chemicals), 1.6 M solution of butyllithiumu in *n*-hexane (Kanto Chemicals), 4-bromophenol (Kanto Chemicals), *tert*-butoxydimethylsilyl chloride (Aldrich), 4-dimethylaminopyridine (Tokyo Kasei), tetrakistriphenylphosphine palladium (Tokyo Kasei), tetra-*n*-butylammonium fluoride (Tokyo Kasei), 10-bromodecanol (Tokyo Kasei), acryloyl chloride (Ardrich) and poly (propyleneimine) dendrimers (G = 1–5) (Aldrich) were purchased and used as received. Trimethyl borate (Tokyo Kasei) was distilled. Tetrahydrofuran (THF) was distilled from sodium-benzophenone ketyl just before use. Unless otherwise noted, the remaining chemicals were commercially available and used without further purification.

4.2.1. 3-Butoxy-1,2-difluorobenzene (2). A solution of 2,3-difluorophenol (35.5 g, 0.250 mol), bromobutane (40.0 ml, 0.375 mol) and K_2CO_3 (51.8 g, 0.375 mol) in 2-butanone (300 ml) was stirred under reflux for 12 h under nitrogen. The resulting suspension was concentrated under reduced pressure, extracted with ether, and the extract then washed with aqueous K_2CO_3 solution ($2.0\,ml^{-1}$) and finally water. The organic layer was dried over $MgSO_4$ and concentrated under reduced pressure. The residue was distilled under reduced pressure to give a colourless liquid; yield 43 g (0.23 mol, 92%), b.p. 54–56°C (1.0 mm Hg). ^1H NMR ($CDCl_3$, 600 MHz): $\delta = 0.98$ (t, $J = 7.20$ Hz, 3H, CH_3), 1.50 (hex, $J =$ 7.20 Hz, 2H, $-CH_2CH_3$), 1.80 (pent, $J = 6.60$ Hz, 2H, $ArOCH_2CH_2-$), 4.03 (t, $J = 6.60$ Hz, 2H, $ArOCH_2$), 6.71–6.76 (m, 2H, ArH), 7.95 (m, 1H, ArH). IR (NaCl): $\nu\,(cm^{-1}) = 1080$, 1250 (C–O–C), 1170 (C–F).

4.2.2. 4-Butoxy-2,3-difluorophenylboronic acid (3). A solution of **2** (23.8 g, 0.128 mol) in THF (130 ml) was cooled to −78°C under nitrogen, and a 1.6 M solution of *n*-butyllithium in *n*-hexane (100 ml, 0.16 mol) added via a cannula; the mixture was stirred at −78°C for 3 h. Trimethyl borate (17.9 ml, 0.160 mol) was slowly added via dropping funnel; the mixture was stirred at room temperature for 24 h, and then poured into aqueous hydrochloric acid (2.0 M, 500 ml). After stirring for 1 h, the aqueous mixture was extracted with benzene. The organic layer was washed with water several times, dried over $MgSO_4$ and concentrated under reduced pressure. The residue was recrystallized from toluene to give white needles (19 g, 82 mmol, 64%). ^1H NMR ($CDCl_3$, 600 MHz): $\delta = 0.99$ (t, $J = 7.20$ Hz, 3H, CH_3), 1.51 (hex, $J = 7.20$ Hz, 2H, $-CH_2CH_3$), 1.82 (pent, $J = 6.60$ Hz, 2H, $ArOCH_2CH_2-$), 4.08 (t, $J = 6.60$ Hz, 2H, $ArOCH_2$), 4.95 (d, 2H, B–OH), 6.78 (ddd, 1H, ArH), 7.48 (ddd, 1H, ArH). IR (NaCl): $\nu\,(cm^{-1}) = 1080$, 1250 (C–O–C), 1170 (C–F), 3300 (O–H).

4.2.3. 4-(*tert*-Butyldimethylsilyloxy)bromobenzene (5). To a solution of 4-bromophenol (17.3 g, 0.100 mol) and 4-dimethylaminopyridine (14.7 g, 0.120 mol) in THF (100 ml), *tert*-butyldimethylsilyl chloride (18.1 g, 0.120 mol) was added dropwise at 0°C. The solution was stirred at room temperature for 1 h; the precipitate was filtered off, and the filtrate concentrated under reduced pressure. The residue was extracted with ether, and the organic layer washed with aqueous K_2CO_3 solution (2.0 M), then with water, dried over $MgSO_4$ and concentrated. The residue was purified by flash column chromatography on SiO_2 with ethyl acetate/*n*-hexane (1/1, v/v) as eluant to give a colourless oil. ^{1}H NMR ($CDCl_3$, 600 MHz): δ (ppm) = 0.18 (s, 6H, Si–CH_3), 0.97(s, 9H, C–CH3), 6.71 (d, 2H, ArH), 7.31 (d, 2H, ArH). IR (NaCl): ν (cm^{-1}) = 780 (Si–C), 1250 (Si–O–C).

4.2.4. 4-Butoxy-2,3-difluoro-4′-hydroxybiphenyl (6). A solution of **5** (11.5 g, 40 mmol) and $Pd(PPh_3)_4$ in benzene (100 ml) was added to a mixture of **3** (10.1 g, 44 mmol) in ethanol (100 ml) and an aqueous solution of K_2CO_3. The resulting mixture was stirred under reflux for 24 h, and poured into water (400 ml). The aqueous mixture was extracted with benzene, and the organic layer was washed with water, dried over $MgSO_4$, and concentrated. The residue was treated with tetra-*n*-butylammonium fluoride in THF for 1 h, and the solvent evaporated. The residue was purified by column chromatography on SiO_2 with *n*-hexane/ethyl acetate (2/3, v/v) as eluant to give a white powder, which was then recrystallized from methanol to give white plates (9.9 g, 35%), m.p. 120–123°C.

4.2.5. 4-Butoxy-2,3-difluoro-4′-(10-hydroxydecyloxy)biphenyl (7). A solution of **6** (5.8 g, 20 mmol), 10-bromodecanol (6.0 ml, 30 mmol), and K_2CO_3 (5.5 g, 40 mmol) in 2-butanone (70 ml) was stirred under reflux for 12 h under nitrogen. The solvent was evaporated, and the residue extracted with ether. The organic layer was washed with water, dried over Na_2SO_4 and concentrated. The resulting solid was recrystallized from methanol to give a white powder (17 mmol, 86%), m.p. 99–101°C.

4.2.6. 4-Butoxy-2,3-difluoro-4′-(10-acryloyloxydecyloxy)biphenyl (8). To a solution of **7** (7.5 g, 17 mmol) and triethylamine in THF, a solution of acryloyl chloride (1.8 ml, 22 mmol) in THF (30 ml) was added dropwise at 0°C. After stirring for 1 h at room temperature, the reaction mixture was concentrated and extracted with ether. The organic layer was washed with water, dried over Na_2SO_4 and concentrated under reduced pressure. The residue was recrystallized from *n*-hexane to give white crystal (6.6 g, 13 mmol, 79%), m.p. 56–57°C.

4.2.7. Preparation of liquid crystalline dendrimers. The typical procedure was as follows: To a solution of polypropyleneimine dendrimer (0.10 mmol) in THF (5.0 ml), a solution of **8** (60 equivalents to the peripheral aminogroups) in THF (5.0 ml) was added. The resulting solution was stirred at 45°C for 1 week under nitrogen and then poured into 300 ml of *n*-hexane. The precipitate was collected by filtration, and the obtained powder purified by reprecipitation with THF/*n*–hexane.

Dendrimer DFD–G1 was prepared from polypropyleneimine dendrimer generation 1 (0.032 g, 0.10 mmol) and **8** (1.17 g, 2.40 mmol); yield 0.43 g (0.098 mmol, 98%). ^{1}H NMR ($CDCl_3$, 600 MHz): δ (ppm) = 0.99 (t, 24H, CH_3), 1.30–1.83 (m, 172H, CH_2), 2.37–2.44 (m, 36H, N–CH_2), 2.77 (t, 16H, N–CH_2), 3.97 (t, 16H, PhOCH_2), 4.03–4.07 (m, 32H, PhOCH_2), 6.76 (m, 8H, ArH), 6.93 (d, 16H, ArH), 7.03 (m, 8H, ArH), 7.40 (d, 16H, ArH). IR (KBr): ν (cm^{-1}) = 1180 (C–F), 1730 (C = O).

Dendrimer DFD–G2 was prepared from polypropyleneimine dendrimer generation 2 (0.077 g, 0.10 mmol) and **8** (2.34 g, 4.80 mmol); yield 0.83 g (0.097 mmol, 97%). ^{1}H NMR ($CDCl_3$, 600 MHz): δ (ppm) = 0.99 (t, 48H, CH_3), 1.30–1.83 (m, 348H, CH_2), 2.37–2.44 (m, 84H, N–CH_2), 2.77 (t, 32H, N–CH_2), 3.97 (t, 32H, ArOCH_2), 4.03–4.07 (m, 64H, PhOCH_2), 6.76 (m, 16H, ArH), 6.93 (d, 32H, ArH), 7.03 (m, 16H, ArH), 7.40 (d, 32H, ArH). IR (KBr): ν (cm^{-1}) = 1180 (C–F), 1730 (C = O).

Dendrimer DFD-G3 was prepared from polypropyleneimine dendrimer generation 3 (0.067 g, 0.04 mmol) and **8** (1.88 g, 3.84 mmol); yield 0.64 g (0.037 mmol, 92%). ^{1}H NMR ($CDCl_3$, 600 MHz): δ (ppm) = 0.97 (t, 96H, CH_3), 1.29–1.81 (m, 700H, CH_2), 2.42 (t, 180H, N–CH_2), 2.76 (t, 64H, N–CH_2), 3.93 (t, 64H, ArOCH_2), 4.02–4.04 (m, 128H, PhOCH_2), 6.73 (m, 32H, ArH), 6.90 (d, 64H, ArH), 7.00 (m, 32H, ArH), 7.37 (d, 64H, ArH). IR (KBr): ν (cm^{-1}) = 1180 (C–F), 1730 (C = O).

Dendrimer DFD-G4 was prepared from polypropyleneimine dendrimer generation 4 (0.070 g, 0.02 mmol) and **8** (3.13 g, 6.40 mmol); yield 0.67 g (0.019 mmol, 97%). ^{1}H NMR ($CDCl_3$, 600 MHz): δ (ppm) = 0.96 (t, 192H, CH_3), 1.28–1.79 (m, 1408H, CH_2), 2.42 (t, 372H, N–CH_2), 2.76 (t, 128H, N–CH_2), 3.90 (t, 128H, ArOCH_2), 3.99–4.03 (m, 256H, PhOCH_2), 6.70 (t, 64H, ArH), 6.87 (d, 128H, ArH), 6.97 (t, 64H, ArH), 7.34 (d, 128H, ArH). IR (KBr): ν (cm^{-1}) = 1180 (C–F), 1730 (C = O).

Dendrimer DFD–G5 was prepared from polypropyleneimine dendrimer generation 5 (0.072 g, 0.01 mmol)

and **8** (3.13 g, 6.40 mmol); yield 0.67 g (0.0096 mmol, 96%). ^{1}H NMR ($CDCl_3$, 600 MHz): δ (ppm) = 0.93 (t, 3842H, CH_3), 1.28–1.74 (m, 2812H, CH_2), 2.43 (s, 756H, N–CH_2), 2.76 (s, 256H, N–CH_2), 3.85–4.02 (m, 768H, ArOCH_2), 6.65 (s, 128H, ArH), 6.83 (s, 256H, ArH), 6.92 (s, 128H, ArH), 7.30 (s, 256H, ArH). IR (KBr): ν (cm^{-1}) = 1180 (C–F), 1730 (C = O).

References

[1] D.A. Tomalia, A.M. Naylor, W.A. Goddard. *Angew. Chem., int. Ed. Engl.*, **29**, 138 (1990).

[2] E.M.M.d.B.-v.d. Berg, E.W. Meijer. *Angew. Chem., int. Ed. Engl.*, **32**, 1308 (1993).

[3] J.M. Frechet. *Science*, **263**, 1710 (1994).

[4] E.I. Ryumtsev, N.P. Evlampieva, A.V. Lezov, S.A. Ponomarenko, N.I. Boiko, V.P. Shibaev. *Liq. Cryst.*, **25**, 475 (1996).

[5] F. Zeng, S.C. Zimmerman. *Chem. Rev.*, **97**, 1681 (1997).

[6] O.A. Matthews, A.N. Shipwa, J.F. Stoddart. *Prog. polym. Sci.*, **23**, 1 (1998).

[7] M. Boxtel, D. Broer, C. Bastiaansen, M. Baars, R. Janssen. *Makromol. Symp.*, **154**, 24 (2000).

[8] D. Patton, M.-K. Park, S. Wang, R.C. Advincula. *Langmuir*, **16**, 1688 (2002).

[9] V. Percec, P. Chu, G. Ungar, J. Zhou. *J. Am. chem. Soc.*, **117**, 11441 (1995).

[10] S.A. Ponomarenko, E.A. Rebrov, A.Y. Bobrovsky, N.I. Boiko, A.M. Muzafarov, V.P. Shibaev. *Liq. Cryst.*, **21**, 1 (1996).

[11] K. Lorenz, D. Holter, B. Stuhn, R. Mulhaupt, H. Frey. **8**, 414 (1996).

[12] P. Busson, H. Ihre, A. Hult. *J. Am. chem. Soc.*, **120**, 9070 (1998).

[13] K. Suzuki, O. Haba, R. Nagahata, K. Yonetake, M. Ueda. *High Perform. Polym.*, **10**, 231 (1998).

[14] K. Yonetake, K. Suzuki, T. Morishita, R. Nagahata, M. Ueda. *High Perform. Polym.*, **10**, 373 (1998).

[15] K. Yonetake, T. Masuko, T. Morishita, K. Suzuki, M. Ueda, R. Nagahata. *Macromolecules*, **32**, 6578 (1999).

[16] O. Haba, K. Okuyama, K. Yonetake. *Mol. Cryst liq. Cryst.*, **364**, 929 (2001).

[17] M.C. Coen, K. Lorenz, J. Kressler, H. Frey, R. Mulhaupt. *Macromolecules*, **29**, 8069 (1996).

[18] A.P.H.J. Schenning, C. Elissen-Roman, J.-W. Weener, M.W.P.L. Baars. *J. Am. chem. Soc.*, **120**, 8199 (1998).

[19] M.W.P.L. Baars, S.H.M. Sontjens, H.M. Fischer, H.W.I. Peerlings, E.W. Meijer. *Chem. Eur. J.*, **4**, 2456 (1998).

[20] R.M. Richardson, S.A. Ponomarenko, N.I. Boiko, V.P. Shibaev. *Liq. Cryst.*, **26**, 101 (1999).

[21] S.A. Ponomarenko, N.I. Boiko, V.P. Shibaev, R.M. Richardson, I.J. Whitehouse, E.A. Rebrov, A.M. Muzafarov. *Macromolecules*, **33**, 5549 (2000).

[22] B. Donnio, J. Barbera, R. Gimenez, D. Guillon, M. Marcos, J.L. Serrano. *Macromolecules*, **35**, 370 (2002).